Journal of Materials Chemistry B

PAPER

View Article Online
View Journal | View Issue

Cite this: J. Mater. Chem. B, 2019, 7, 5775

A selective cascade reaction-based probe for colorimetric and ratiometric fluorescence detection of benzoyl peroxide in food and living cells†

Xiaoli Wu,[a] Lintao Zeng,[ab] Bao-Quan Chen,[a] Ming Zhang,*[a] João Rodrigues,[c] Ruilong Sheng *[c] and Guang-Ming Bao *[d]

Received 6th May 2019,
Accepted 2nd September 2019

DOI: 10.1039/c9tb00889f

rsc.li/materials-b

A novel colorimetric and ratiometric fluorescent probe (**Cou-BPO**) was readily prepared for specific detection of harmful benzoyl peroxide (BPO). The probe **Cou-BPO** reacted with BPO *via* a selective oxidation cleavage-induced cascade reaction of the pinacol phenylboronate group, which resulted in an observable colorimetric and ratiometric fluorescence response towards BPO with a fast response time (<15 min) and a low detection limit (56 nM). For practical application, facile, portable and sensitive test paper of **Cou-BPO** has been prepared for visual detection of BPO. Furthermore, we employed **Cou-BPO** as a probe to determine BPO in food samples and living cells.

Introduction

Benzoyl peroxide (BPO) has been widely used as an additive during food processing due to its good bleaching properties.[1–4] It has been revealed that excessive BPO in food (*e.g.* wheat flour) would generate highly hazardous oxidizing free radicals and convert into toxic substances such as biphenyl and phenylbenzoate, which might further result in tissue damage and cause diseases.[5–9] Thus, it is indispensible to develop fast and efficient methods for determining BPO in food samples.[10] During the past decades, some analytical approaches have been employed for the detection of BPO, including chemiluminescence,[5,11] amperometry,[4] electrochemistry,[12,13] spectrophotometry[14–17] and high-performance liquid chromatography.[18,19] Nevertheless, these traditional methods have some shortcomings such as low sensitivity, and the requirement for expensive analytical instruments and elaborate sample treatment processes.

Fluorescent probes have been employed as powerful detection tools for various chemical species due to their advantages of high sensitivity and selectivity, quick response, high spatial resolution, and real-time detection.[20–25] However, to date, only a few fluorescent probes have been explored for the detection of BPO. For instance, Ma *et al.* developed a fluorescence off–on type probe for sensing BPO based on resorufin.[16] Yang *et al.* developed a near-infrared fluorescent probe for sensing/imaging BPO in zebrafish.[26] Nevertheless, these probes have restrictions associated with probe distribution, environmental conditions and the efficiency of instruments.[27,28] By contrast, ratiometric fluorescent probes are able to achieve more accurate analysis results by offering a built-in correction.[29–36] Li *et al.* developed a phenylboronic acid pinacol ester-containing fluorescent probe for determining BPO with good selectivity and sensitivity in food samples.[37] In prior research, we devised a ratiometric fluorescent probe for BPO on the basis of an oxidation cleavage reaction of an alkene group (the C=C bond/bridge).[10] Although progress has been achieved, it is still highly desired to develop some new and inexpensive fluorescent probes for sensing BPO with the advantages of being easy-to-prepare, and having long wavelength emission, a visible color change, a short response time, and good selectivity and sensitivity.

7-Alkylamino-coumarin possesses a high fluorescence quantum yield and large Stokes shift, as well as good photostability and low cytotoxicity.[38,39] Herein, we used 7-diethylamino-coumarin to prepare a novel probe **Cou-BPO** for sensing BPO. The optical responses of **Cou-BPO** to BPO were investigated by UV-vis and fluorescence spectroscopy. ^{1}H NMR and HR-MS spectra were employed to investigate the reaction between

[a] Tianjin Key Laboratory of Organic Solar Cells and Photochemical Conversion, Tianjin University of Technology, Tianjin 300384, P. R. China. E-mail: zlt1981@126.com, zm2404@tjut.edu.cn
[b] Department of Chemsitry and Materials Science, Hubei Engineering University, Hubei Xiaogan 432100, P. R. China
[c] CQM-Centro de Química da Madeira, Universidade da Madeira, Campus da Penteada, 9000-390, Funchal, Madeira, Portugal. E-mail: ruilong.sheng@staff.uma.pt
[d] Institute of Veterinary Drug/Jiangxi Provincial Key Laboratory for Animal Health, Jiangxi Agricultural University, Nanchang, 330045, P. R. China. E-mail: bycb2005@gmail.com

† Electronic supplementary information (ESI) available: Fluorescence spectra, cytotoxicity, cell imaging, and NMR and HR-MS spectra. See DOI: 10.1039/c9tb00889f

Cou-BPO and BPO, and the working mechanism was proposed. Furthermore, facile to use, portable and sensitive test paper of **Cou-BPO** has been prepared. For practical application, we attempted to employ the probe **Cou-BPO** for determining BPO in food (wheat flour and noodle) samples. Finally, **Cou-BPO** was further employed for visually detecting and imaging BPO in living cells. This probe exhibited some remarkable features including a large Stokes shift, good solubility, excellent selectivity and sensitivity, and a ratiometric fluorescence response towards BPO.

Results and discussion

Design and synthesis of probe Cou-BPO

The fluorescence spectrum of coumarin could be modulated by three means: (1) introducing electron-donor groups (EDG, such as –OH and $-Et_2N$) at the 7-position; and (2) introducing electron-withdrawing groups (EWG, such as pyridinium and indolium) or (3) extending the π-conjugation system at the 3-position. In this work, we employed 7-diethylaminocoumarin-3-aldehyde as the fluorophore, which was covalently conjugated with 4-methyl-1-(4-boronic acid pinacol ester)benzyl pyridinium to form the probe **Cou-BPO** with an intramolecular charge transfer feature (Scheme 1). The structure of **Cou-BPO** was fully characterized by ^{1}H and ^{13}C NMR, as well as HR-MS (Fig. S1–S4, ESI†). It could be envisioned that **Cou-BPO** will display deep red emission due to the typical intramolecular charge transfer (ICT) feature. In the presence of BPO, the pinacol phenylboronate group on **Cou-BPO** might be cleaved by BPO-induced oxidation, followed by elimination of *p*-quinone methide to eventually generate a new 7-diethylaminocoumarin derivative, which may cause significant changes of the absorption/fluorescence spectra.

Sensing properties of Cou-BPO towards BPO

To investigate the sensing properties of **Cou-BPO** towards BPO, we performed the UV-vis absorption and fluorescence spectral titration of probe **Cou-BPO** (10 μM) with various amounts of BPO. As shown in Fig. 1A, upon the addition of increasing amounts of BPO (0–150 μM), the UV-vis absorption band of **Cou-BPO** centered at 505 nm decreased gradually accompanied by a new absorption peak at 443 nm gradually increasing. Consequently, the **Cou-BPO** solution exhibited an obvious color change from red to yellow (Fig. 1A and B, inset). By plotting the absorbance at 443 nm (A_{443}) *versus* the concentration of BPO, a good linear relationship (R^2 = 0.9905) between A_{443} and the BPO concentration could be observed (Fig. 1B). Meanwhile, the fluorescence emission band at 620 nm of **Cou-BPO** gradually decreased and a new emission peak appeared at 525 nm.

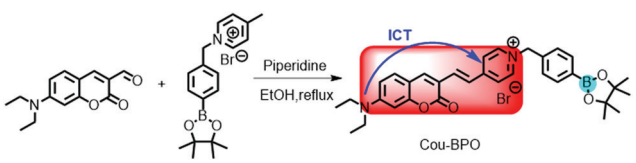

Scheme 1 The synthetic route of probe **Cou-BPO**.

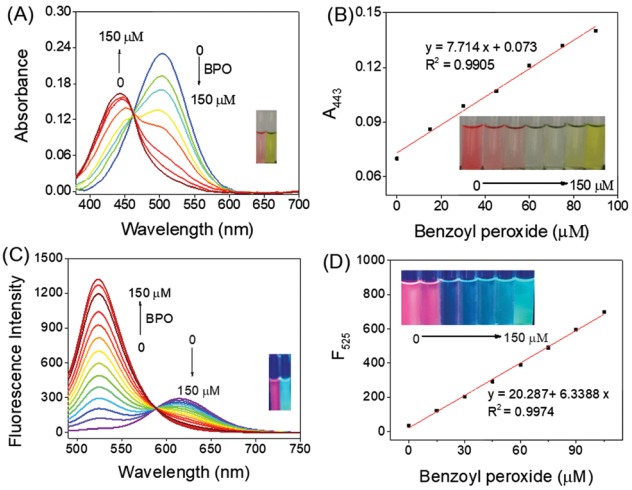

Fig. 1 (A) UV-vis absorption and (C) fluorescence spectrum changes of **Cou-BPO** (10 μM) in EtOH in the presence of BPO (0–150 μM); (B) linear relationship between the absorbance of **Cou-BPO** and concentration of BPO. (D) Fluorescence intensity of **Cou-BPO** *versus* concentration of BPO. λ_{ex} = 480 nm, λ_{em} = 525 nm, slit widths: 2.5 nm/2.5 nm.

Consequently, the fluorescence color changed from red to green (Fig. 1C), which could be easily observed with the naked eye. The fluorescence spectra of **Cou-BPO**, **Cou-BPO**/BPO and their coumarin precursors are shown in Fig. S5 (ESI†). Moreover, the fluorescence quantum yield of **Cou-BPO** (Φ = 0.12, in EtOH) was enhanced (Φ = 0.18, in EtOH) after reaction with BPO, thus giving rise to strong green fluorescence which was clearly visible to the naked eye. Moreover, the fluorescence intensity F_{525}/F_{620} is linearly related to the BPO concentration (Fig. 1D, R^2 = 0.9974), and the detection limit for BPO was calculated to be 56 nM (S/N = 3).

The response time is an important parameter for the practical application of a probe. Thus, the time-dependent fluorescence spectrum of **Cou-BPO** (10 μM) towards BPO (15 equiv.) was measured and recorded every 30 s. As shown in Fig. 2, the fluorescence intensity at 525 nm increased rapidly after the addition of BPO and reached a plateau within 13 min, along with the gradual decrease of the fluorescence intensity at 620 nm, suggesting that **Cou-BPO** could be employed as a fast

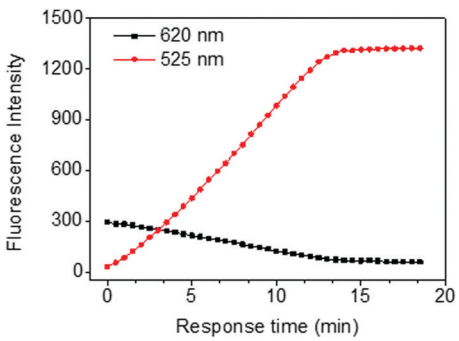

Fig. 2 Fluorescence intensity changes of **Cou-BPO** (10 μM) after addition of BPO (150 μM) at different time intervals.

sensing tool to determine low concentrations of BPO in practical application.

To evaluate the selectivity of **Cou-BPO** towards BPO, we examined the ratiometric fluorescence response of **Cou-BPO** (F_{525}/F_{620}) towards various anionic, cationic and small molecule analytes (150 μM). As shown in Fig. 3, **Cou-BPO** displayed an obvious color change from red to yellow together with a fluorescence change from red to green in the presence of BPO (Fig. 3, inset). The addition of ClO^- or H_2O_2 quenched the fluorescence of the probe, and **Cou-BPO** did not exhibit an observable fluorescence response towards some other anionic analytes like I^-, F^-, Cl^-, Br^-, AcO^-, CO_3^{2-}, HCO_3^-, $S_2O_3^{2-}$, SO_3^{2-}, SO_4^{2-}, NO_3^-, N_3^-, TBHP, $TBO^\bullet$, $^1O_2$, $^\bullet O_2^-$, $^\bullet OH$, GSH, HS^-, HSO_3^-, Hcy and Cys. Besides, the cationic and small molecule analytes do not bring about observable fluorescence changes. These results demonstrate that **Cou-BPO** is a highly selective fluorescent probe for BPO among common anionic, cationic and small molecule analytes.

Sensing mechanism of Cou-BPO towards BPO

To investigate the sensing mechanism of **Cou-BPO** towards BPO, the reaction product of **Cou-BPO** with the addition of excess BPO was identified by HR-MS (Fig. S6, ESI†). The HR-MS result showed that an obvious signal peak appeared at *m*/*z* 321.3158, which was assigned to 7-(diethylamino)-3-(2-(pyridin-4-yl)vinyl)-coumarin (compound **3**). From the results, the reaction mechanism could be deduced as: BPO firstly reacts with the pinacol phenylboronate on **Cou-BPO** to produce a phenol, which then underwent a spontaneous quinone methide elimination reaction to generate 7-(diethylamino)-3-(2-(pyridin-4-yl)vinyl)-coumarin. The probe **Cou-BPO** showed strong red-fluorescence emission due to its strong ICT effect. By contrast, the ICT effect in compound **3** was largely diminished by conversion of the stronger electro-withdrawing pyridium group on **Cou-BPO** into the weaker electro-withdrawing pyridine group *via* *p*-quinone methide elimination, which subsequently gave rise to an obvious blue-shift of the fluorescence emission. Moreover, it could be noted that compound **3** is relatively stable and inert towards excess BPO. The proposed sensing mechanism is shown in Scheme 2.

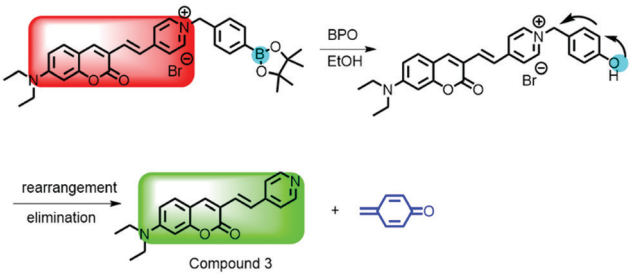

Scheme 2 Sensing mechanism of **Cou-BPO**.

To verify that the BPO-involved selective oxidation did not occur on the C=C bond/bridge located between the coumarin and the pyridine rings, a model compound **Cou-Pyr** was synthesized and characterized by ^{1}H NMR and HR-MS (Fig. S7 and S8, ESI†). After addition of excess BPO, the UV-vis absorption spectra (Fig. S9, ESI†), fluorescence spectra (Fig. 4A) and time-resolved fluorescence response (Fig. 4B) of **Cou-Pyr** showed no obvious change, implying that model compound **3** is inert to BPO. In our previous research, we found that BPO could react with the C=C bond/bridge of (7-diethylamino coumarin-3-yl)vinyl)-1-ethyl-3,3-dimethyl-3*H*-indolium *via* BPO-induced oxidation cleavage, affording blue fluorescent 7-diethylamino coumarin-3-aldehyde.[10] Interestingly, in this work, the BPO-induced oxidation reaction only occurred on the site of pinacol phenylboronate instead of the C=C bond/bridge. By contrast to **Cou-BPO**, the model compound **Cou-Pyr** is very stable and inert to BPO oxidation, which is probably due to its less polarized "push–pull" structure that stabilized the conjugation system. The reactivity difference between **Cou-BPO** and **Cou-Pyr** is shown in Scheme 3. These results indicated that **Cou-BPO** could react with BPO *via* a selective oxidation cleavage-induced cascade reaction, which may benefit the design and synthesis of a "site-selective" chemodosimeter for sensing application.

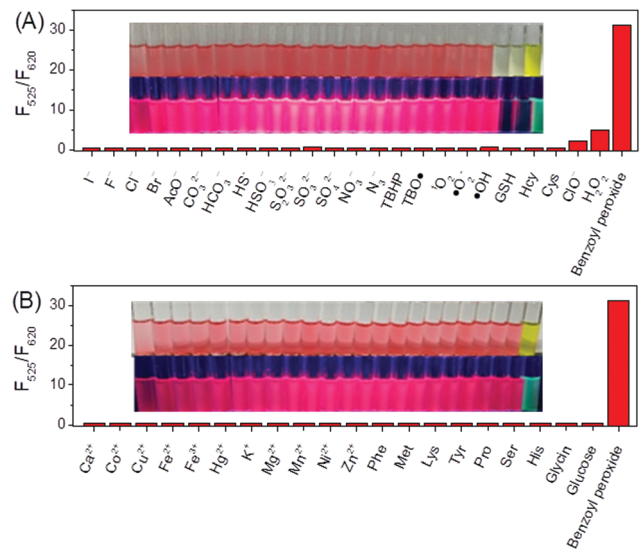

Fig. 3 Fluorescence intensity ratios (F_{525}/F_{620}) of **Cou-BPO** (10 μM) in the presence of BPO (150 μM) and other analytes (150 μM) for 15 min: (A) I^-, F^-, Cl^-, Br^-, AcO^-, CO_3^{2-}, HCO_3^-, HS^-, HSO_3^-, $S_2O_3^{2-}$, SO_3^{2-}, SO_4^{2-}, NO_3^-, N_3^-, TBHP, $TBO^\bullet$, $^1O_2$, $^\bullet O_2^-$, $^\bullet OH$, GSH, Hcy, Cys, ClO^-, H_2O_2, and benzoyl peroxide. (B) Ca^{2+}, Co^{2+}, Cu^{2+}, Fe^{2+}, Fe^{3+}, Hg^{2+}, K^+, Mg^{2+}, Mn^{2+}, Ni^{2+}, Zn^{2+}, Phe, Met, Lys, Tyr, Pro, Ser, His, glycine, glucose, and benzoyl peroxide. Inset: The color and fluorescence images of **Cou-BPO** in EtOH with different analytes.

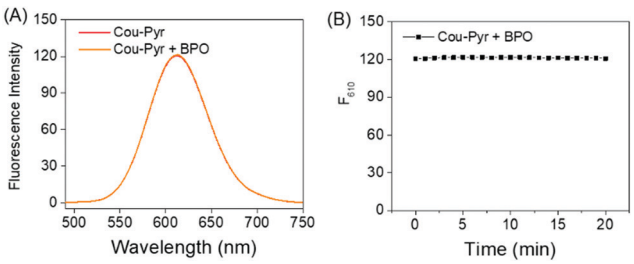

Fig. 4 (A) Fluorescence spectra of **Cou-Pyr** (10 μM) with BPO (150 μM) in EtOH solution. (B) Time-resolved fluorescence responses of **Cou-Pyr** (10 μM) towards BPO (150 μM). λ_{ex} = 490 nm, λ_{em} = 610 nm, slit widths = 2.5 nm/5 nm.

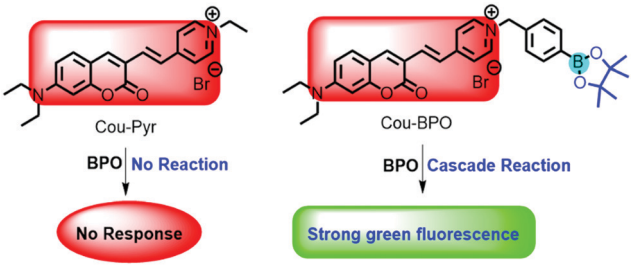

Scheme 3 Reactivity of the probe **Cou-BPO** and model compound **Cou-Pyr** towards BPO.

Test paper of Cou-BPO

For fast and portable detection of BPO, filter paper strips were soaked in **Cou-BPO** (1 mM) and then dried in air to prepare **Cou-BPO** test paper. After exposure to different amounts of BPO (0–150 μM) for 15 min (Fig. 5), the fluorescence color of the **Cou-BPO** test paper changed from bright-red to grey and then to olive-green. In the food industry, BPO was used as an oxidizing agent for bleaching and wheat flour decolorization. Earlier publications have disclosed that BPO intake can cause oxidative cell/tissue damage; the above results showed that the **Cou-BPO** test paper was able to detect trace amounts of BPO within the harmful range (0–70 μM).[5] Herein we examined the **Cou-BPO** test paper for determination of BPO in the EtOH extracts of two food samples (wheat flour and noodles produced in Tianjin, China). As shown in Fig. 6, the bright red color of the **Cou-BPO** test paper was still maintained in the presence of BPO; simultaneously, no obvious fluorescence color change could be observed, indicating that a negligible amount of BPO exists in these test food samples. These semi-quantitative results suggested that the **Cou-BPO** test paper may serve as a highly selective test kit for real-time detection of BPO in wheat flour-based food samples.

Determination of BPO in real food samples by using Cou-BPO

On the basis of the excellent sensitivity and selectivity of **Cou-BPO** toward BPO, we further attempted to examine the applicability of **Cou-BPO** for quantitative determining BPO in these samples. The BPO in these real food samples was firstly extracted with EtOH and then a predetermined amount of BPO

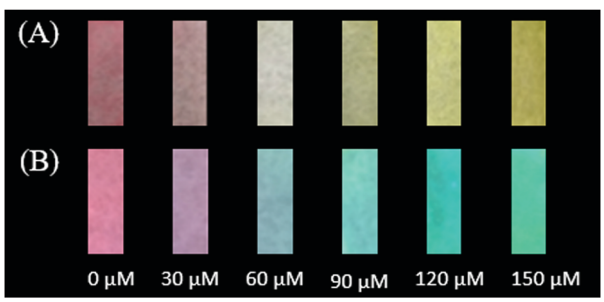

Fig. 5 Photos of (A) color and (B) fluorescence of **Cou-BPO** test paper after exposure to different amounts of BPO (0–150 μM) under 365 nm light.

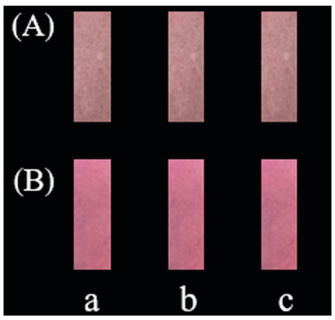

Fig. 6 Photos of (A) color and (B) fluorescence of **Cou-BPO** test paper after exposure to the EtOH extracts of food samples (a, blank; b, wheat flour; c, noodles).

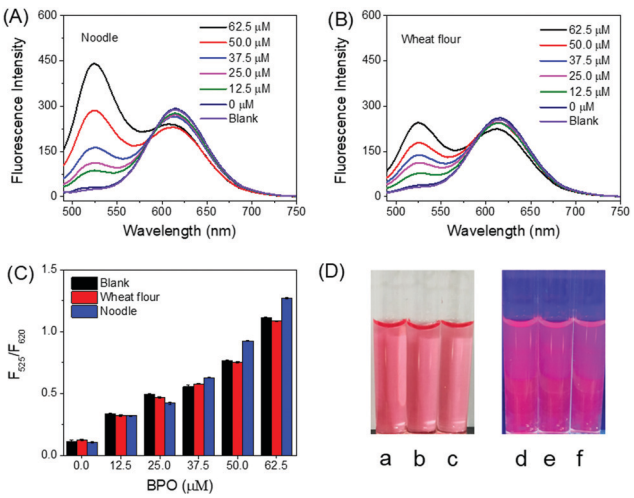

Fig. 7 Fluorescence spectrum changes of **Cou-BPO** (10 μM) in noodle (A) and wheat flour (B) solutions. λ_{ex} = 480 nm, λ_{em} = 525 nm, slit widths = 2.5 nm/2.5 nm. (C) Fluorescence intensity ratios (F_{525}/F_{620}) of **Cou-BPO** (10 μM) in the presence of the BPO in the food sample solutions. (D) The color and fluorescence images of **Cou-BPO** in the presence of different food samples (a and d: blank; b and e: wheat flour; c and f: noodles). n = 3.

(0, 12.5 μM, 25.0 μM, 37.5 μM, 50.0 μM, and 62.5 μM) was spiked into the samples. As shown in Fig. 7, no obvious fluorescence enhancement was observed in the blank (none-BPO spiked) food samples, indicating that a negligible amount of BPO exists in the two food samples. With the increase of the spiked BPO, obvious fluorescence enhancement at 525 nm was observed along with a fluorescence decrease at 620 nm. According to the standard calibration curve in Fig. 1D, the amounts of BPO in the wheat flour and noodle samples were determined. However, comparatively low–medium recoveries (30.4–66.7%) were obtained (Table 1). It could be noted that the boronate group could selectively bind to the hydroxyl groups in the starch chain, and thus may interfere with the high selectivity of **Cou-BPO** toward BPO in food samples.

Fluorescence imaging of BPO in living cells by using Cou-BPO

To visualize BPO in living cells, firstly, the cytotoxicity of **Cou-BPO** (2.5, 5.0, 10.0, 15.0, 20.0, and 25.0 μM) in murine

Table 1 Determination of BPO by **Cou-BPO** in food samples

Sample	Added (μM)	Found (μM)	Recovery (%)	RSD (%)
Wheat flour	12.5	5.46	40.89	1.8
	25.0	9.02	34.87	1.1
	37.5	11.70	30.49	1.7
	50.0	15.93	31.33	0.6
	62.5	22.53	35.57	1.3
Noodles	12.5	6.48	48.96	3.1
	25.0	8.83	34.31	2.3
	37.5	14.25	37.26	0.7
	50.0	26.98	53.17	1.1
	62.5	42.22	66.75	0.3

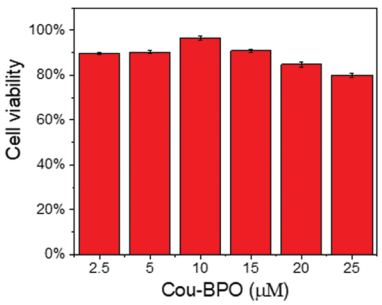

Fig. 8 Cytotoxicity of **Cou-BPO** at various concentrations (2.5 μM, 5.0 μM, 10.0 μM, 15.0 μM, 20.0 μM, and 25.0 μM) towards L929 cells for 24 h. The results are the mean and standard deviation of five separate measurements. Error bars are ± SD, n = 5.

fibroblast L929 cells was evaluated by using a CCK-8 assay kit. As shown in Fig. 8, the L929 cell viability remained at 80.6–96.8% after incubation with 2.5–25 μM **Cou-BPO** for 24 h, indicating that **Cou-BPO** has low cytotoxicity and good biocompatibility. Then the fluorescence imaging of BPO in living L929 cells was performed. As shown in Fig. 9, red fluorescence was observed (λ_{ex} = 543 nm, red channel) within the cells after incubation with **Cou-BPO** (10 μM) for 30 min. When they were further incubated with different amounts of BPO (0, 25, 50, and 100 μM) for another 30 min, the red fluorescence gradually decreased and eventually disappeared, meanwhile, clear cell images with green fluorescence were observed from the green channel (λ_{ex} = 488 nm). The probe **Cou-BPO** also can image BPO in HeLa (human cervical cancer) cells with good performance (Fig. S10 and S11, ESI†). The results indicated that **Cou-BPO** may serve as an efficient probe for imaging BPO in living cells.

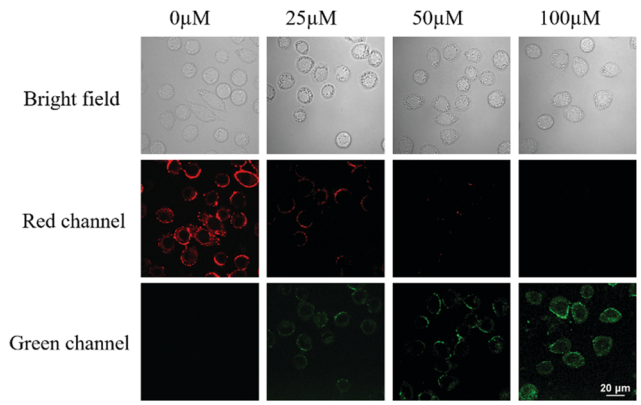

Fig. 9 Fluorescence images of BPO in L929 cells. L929 cells were incubated with **Cou-BPO** (10 μM) at 37 °C for 30 min, and then further treated with various concentrations of BPO (0, 25, 50, and 100 μM). Fluorescence images of L929 cells were obtained from the red channel (λ_{ex} = 543 nm, λ_{em} = 552–617 nm), and green channel (λ_{ex} = 488 nm, λ_{em} = 500–530 nm). Scale bar: 20 μm.

Experimental

Materials and reagents

All reagents were purchased from Sigma-Aldrich and used as received. Chromatographic grade ethanol was used for spectral analysis.

Instruments

A Bruker DPX 400 NMR spectrometer was employed to determine the ^{1}H and ^{13}C NMR spectra using tetramethylsilane (TMS) as an internal standard. High-resolution mass spectra (HR-MS) were obtained with a HP-1100 LC-MS spectrometer. UV-vis absorption and fluorescence spectra were measured with a Hitachi UV-3310 spectrometer and a Hitachi FL-4500 fluorometer, respectively.

Synthesis procedures of Cou-BPO

7-Diethylaminocoumarin-3-aldehyde (300 mg, 1.22 mmol), and 4-methyl-1-(4-boronic acid pinacol ester) benzyl pyridinium bromide (572.6 mg, 1.47 mmol) were placed in a flask with 10 mL EtOH as the solvent and 0.05 mL (0.54 mM) piperidine as the catalyst. The mixture was refluxed for 5 h under a nitrogen atmosphere, and then the solvent was removed by vacuum evaporation. The crude product was purified by silica gel column chromatography (CH_2Cl_2 : MeOH = 8 : 1 as the eluent) to give **Cou-BPO** as a dark red solid (250 mg, yield: 45%).^{1}H NMR (400 MHz, DMSO-d_6) δ 8.97 (d, J = 6.8 Hz, 2H), 8.25 (s, 1H), 8.20 (d, J = 6.4 Hz, 2H), 7.90–7.83 (m, 1H), 7.73 (dd, J = 17.0, 15.4 Hz, 3H), 7.54 (dd, J = 15.6, 8.4 Hz, 3H), 6.81 (d, J = 11.2 Hz, 1H), 6.62 (s, 1H), 5.75 (s, 2H), 3.50 (q, J = 6.67 Hz, 4H), 1.29 (s, 12H), 1.15 (t, J = 7.0 Hz, 6H). ^{13}C NMR (100 MHz, DMSO-d_6) δ 152.5, 146.1, 144.5, 138.2, 137.9, 135.6, 131.3, 128.5, 124.1, 122.9, 114.1, 110.5, 108.8, 96.7, 84.3, 56.4, 44.1, 25.1, 12.8. HR-MS (ESI) m/z calculated for $[C_{33}H_{38}BN_2O_4]^+$, 537.2992; found 537.2960 (Fig. S1–S3, ESI†).

General procedure for the detection of BPO

Unless otherwise indicated, all the measurements were performed with the following procedure. **Cou-BPO** (10 μM) solution was prepared by using chromatographic grade EtOH as the test solution. The UV-vis absorption and fluorescence spectra of **Cou-BPO** were recorded after incubation with BPO at 25 °C for 15 min. For comparison, **Cou-BPO** solution (10 μM) without BPO was tested under the same conditions.

Preparation of the test paper

Filter paper was cut into strips (0.8 × 2.4 cm), which were then immersed in 1 mM **Cou-BPO** in EtOH. The probe-soaked filter paper was taken out, and dried naturally overnight. These paper strips were directly used to detect BPO. The supernatants of the food (wheat flour and noodle) samples were dropped onto the test paper for 30 min. The fluorescence photographs of the **Cou-BPO** paper were recorded under 365 nm light.

Determination of BPO in real food samples

Each food sample (4.0 g) and EtOH (40 mL) were put into a beaker and sonicated for 30 min. Each solution was transferred to a 50 mL test tube, and centrifuged for 10 min. The supernatant was collected and then filtered with an organic membrane (0.45 μm). These solutions were spiked with BPO (0, 12.5, 25.0, 37.5, 50.0 and 62.5 μM). Finally, **Cou-BPO** (10 μM) was added to each food sample solution and then the fluorescence spectra were measured on a Hitachi FL-4500 fluorometer.

Cytotoxicity of Cou-BPO and fluorescence imaging of BPO in living cells

The related experimental procedures are described in S1 and S2 (ESI†).

Conclusion

In conclusion, we have prepared a cascade reaction-based fluorescent probe **Cou-BPO** for the detection of BPO, which displayed significant colorimetric and ratiometric fluorescence responses towards BPO with the merits of visual detection, high selectivity and sensitivity, a fast response (within 15 min) and a low limit of detection (56 nM). For practical application, facile, portable and sensitive test paper of **Cou-BPO** has been prepared for visual detection of BPO. Furthermore, we attempted to employ **Cou-BPO** as a probe to determine BPO in food samples and to image/visualize BPO in living cells. This work may provide new insight for developing fast and inexpensive ''sensing site-selective'' probes for sensing various analytes.

Conflicts of interest

All authors of this work declare no research conflict.

Acknowledgements

This work was financially supported by the National Natural Science Foundation of China (No. 21978222, 31960720, 31560712) and the Natural Science Foundation of Tianjin (No. 17JCYBJC19600, 18JCYBJC94900, 18JCTPJC48600). Ruilong Sheng and João Rodrigues appreciate the support from Fundação para a Ciência e a Tecnologia (FCT project PEst-OE/QUI/UI0674/2019, CQM, Portuguese government funds) and ARDITI-Agência Regional para o Desenvolvimento da Investigação Tecnologia e Inovação through the project M1420-01-0145-FEDER-000005-Centro de Química da Madeira-CQM+ (Madeira 14-20 Program) and ARDITI-2017-ISG-003.

Notes and references

1 K. Ponhong, S. A. Supharoek, W. Siriangkhawut and K. Grudpan, *J. Food Drug Anal.*, 2015, **23**, 652–659.
2 L. Chu and F. Qing, *Chem. Commun.*, 2010, **46**, 6285–6287.
3 K. Matyjaszewski and J. Xia, *Chem. Rev.*, 2001, **101**, 2921–2990.
4 J. V. B. Kozan, R. P. Silva, S. H. P. Serrano, A. W. O. Lima and L. Angnes, *Biosens. Bioelectron.*, 2010, **25**, 1143–1148.
5 G. Mu, H. Liu, Y. Gao and F. Luan, *J. Sci. Food Agric.*, 2012, **92**, 960–964.
6 W. Liu, Z. Zhang and L. Yang, *Food Chem.*, 2006, **95**, 693–698.
7 J. Hu, Y. Dong, H. Zhang, X. Chen, X. Chen, H. Zhang and H. Chen, *RSC Adv.*, 2013, **3**, 26307–26312.
8 S. R. Feldman, J. Tan, Y. Poulin, T. Dirschka, N. Kerrouche and V. Manna, *J. Am. Acad. Dermatol.*, 2011, **64**, 1085–1091.
9 Y. Sun, J. Yuan, J. Pang, X. Li, S. Wang, Y. Zhou, F. Xu, P. C. H. Li, S. Jiang and H. Chen, *Talanta*, 2018, **179**, 719–725.
10 Q. Hu, W. Li, C. Qin, L. Zeng and J.-T. Hou, *J. Agric. Food Chem.*, 2018, **66**, 10913–10920.
11 W. Yang, Z. Zhang and X. Hun, *Talanta*, 2004, **62**, 661–666.
12 T. Lin, M. Zhang, F. Xu, X. Wang, Z. Xu and L. Guo, *Sens. Actuators, B*, 2018, **261**, 379–384.
13 Z. Jiang, G. Wen, Y. Luo, X. Zhang, Q. Liu and A. Liang, *Sci. Rep.*, 2015, **4**, 5323.
14 S. Supharoek, K. Ponhong and K. Grudpan, *Talanta*, 2017, **171**, 236–241.
15 X. Wang, C. Zhao, W. Huang, Q. Wang, C. Liu and G. Yang, *Spectrosc. Lett.*, 2017, **50**, 364–369.
16 W. Chen, Z. Li, W. Shi and H. Ma, *Chem. Commun.*, 2012, **48**, 2809–2811.
17 J. Qin, M. Kim, K. Chao, M. Gonzalez and B. K. Cho, *Appl. Spectrosc.*, 2017, **71**, 2469–2476.
18 Y. Chen, P. Tsai, Y. Huang and P. Wu, *PLoS One*, 2015, **10**, 1–9.
19 Y. Abe-Onishi, C. Yomota, N. Sugimoto, H. Kubota and K. Tanamoto, *J. Chromatogr. A*, 2004, **1040**, 209–214.
20 Y. V. Suseela, N. Narayanaswamy, S. Pratihar and T. Govindaraju, *Chem. Soc. Rev.*, 2018, **47**, 1098–1131.
21 C. Duan, J.-F. Zhang, Y. Hu, L. Zeng, D. Su and G.-M. Bao, *Dyes Pigm.*, 2019, **162**, 459–465.
22 Q. Hu, C. Qin, L. Huang, H. Wang, Q. Liu and L. Zeng, *Dyes Pigm.*, 2018, **149**, 253–260.
23 D. Wu, L. Chen, W. Lee, G. Ko, J. Yin and J. Yoon, *Chem. Rev.*, 2018, **354**, 74–97.
24 W. Zhang, T. Liu, F. Huo, P. Ning, X. Meng and C. Yin, *Anal. Chem.*, 2017, **89**, 8079–8083.
25 X. Tian, Z. Li, Y. Pang, D. Li and X. Yang, *J. Agric. Food Chem.*, 2017, **65**, 9553–9558.
26 Y. Yang, F. Huo, C. Yin, M. Xu, Y. Hu, J. Chao, Y. Zhang, T. E. Glass and J. Yoon, *J. Mater. Chem. B*, 2016, **4**, 5101–5104.
27 L. Yuan, W. Lin, Y. Xie, B. Chen and J. Song, *Chem. – Eur. J.*, 2012, **18**, 2700–2706.

28 C. Zhao, X. Zhang, K. Li, S. Zhu, Z. Guo, L. Zhang, F. Wang, Q. Fei, S. Luo, P. Shi, H. Tian and W. Zhu, *J. Am. Chem. Soc.*, 2015, **137**, 8490–8498.
29 J. Xu, J. Pan, X. Jiang, C. Qin, L. Zeng, H. Zhang and J. Zhang, *Biosens. Bioelectron.*, 2016, **77**, 725–732.
30 L. Zhu, J. Xu, Z. Sun, B. Fu, C. Qin, L. Zeng and X. Hu, *Chem. Commun.*, 2015, **51**, 1154–1156.
31 W. Lu, P. Xiao, Z. Liu, J. Gu, J. Zhang, Y. Huang, Q. Huang and T. Chen, *ACS Appl. Mater. Interfaces*, 2016, **8**, 20100–20109.
32 C. Duan, M. Won, P. Verwilst, J. Xu, H. S. Kim, L. Zeng and J. S. Kim, *Anal. Chem.*, 2019, **91**, 4172–4178.
33 F. Wang, C. Zhang, X. Qu, S. Cheng and Y. Xian, *Biosens. Bioelectron.*, 2019, **126**, 96–101.
34 H. Zhang, F. Huo, Y. Zhang and C. Yin, *Sens. Actuators, B*, 2018, **269**, 180–188.
35 Y. Yue, F. Huo, P. Yue, X. Meng, J. C. Salamanca, J. O. Escobedo, R. M. Strongin and C. Yin, *Anal. Chem.*, 2018, **90**, 7018–7024.
36 L. Wang, Q. Zang, W. Chen, Y. Hao, Y. Liu and J. Li, *RSC Adv.*, 2013, **3**, 8674–8676.
37 Z. Xu, X. Liu, J. Pan and D. R. Spring, *Chem. Commun.*, 2012, **48**, 4764–4766.
38 R. Sheng, J. Ma, P. Wang, W. Liu, J. Wu, H. Li, X. Zhuang, H. Zhang and S. Wu, *Biosens. Bioelectron*, 2010, **26**, 949–952.
39 Y. Yue, F. Huo, P. Ning, Y. Zhang, J. Chao, X. Meng and C. Yin, *J. Am. Chem. Soc.*, 2017, **139**, 3181–3185.